Smooth Rolling Morton Knots

Max Brodeur
Geometric Computing Laboratory, EPFL.

June 7, 2024

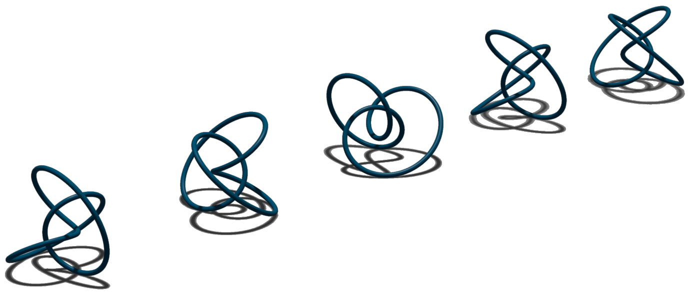

Abstract

The oloid is famous for its mesmerizing rolling behavior. It is less known however, that it is a member of larger family of rolling objects: the Two Disk Rollers. A simple z-coordinate scaling can be applied to Morton's tritangentless knots (Morton, 1991) to obtain TDR convex hulls. Even more, the TDRs have a subfamily with constant center of mass height when rolled (Engelhardt and Ucke, 2017). The z-scaled knots can be projected to these TDRs, yielding smooth rolling knots. Even more, the same process can be applied to a generalization of Morton's knots.

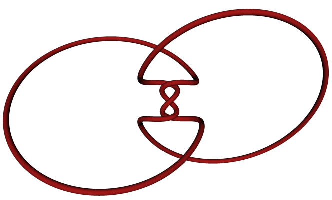

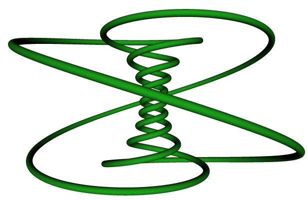

Introduction

Apart from classic circular solids like spheres or cylinders, what other geometry rolls? Enter the *developable rollers*; a class of fantastic new shapes with very interesting properties. The first and most famous of these shapes are the *oloid* and *sphericon*, both defined by the convex hulls of orthogonal circles and half circles respectively. Most relevant to this research are the families of developable rollers these objects belong to. David Hirsch, the sphericon's inventor, showed his roller to be a member of the larger *Polycon* family (Hirsch and Seaton, 2020). However the oloid's family, the Two Disk Rollers (TDR), was defined independently from the oloid. They encompass a much larger collection of rolling objects, all defined by orthogonal disks. The intrigued should read (Engelhardt and Ucke, 2017) for an in-depth enumeration of these objects.

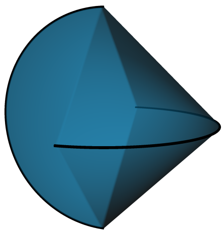

Figure 4: Sphericon

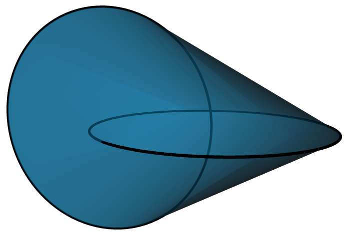

Figure 5: Oloid

As proposed in (Eget, Lucas and Taalman, 2020), one can quantify the smoothness of an object's rolling behavior by computing the range of the height of its center of mass across the rolling trajectory. Here, this metric is referred to as *rolliness* and denoted by ρ.

A smooth rolling object is considered to have $\rho = 0$, like a sphere, since its center of mass height remains constant. The previously mentioned sphericon and its family have the interesting property that they roll smoothly. Even more, as shown in (Engelhardt and Ucke, 2017), a sub family of the Two Disk Rollers roll smoothly when their disk radii and distances satisfy a *zero-rolliness* condition.

Now what about knots? Although most work in knot theory has been about the classification of their topology, this paper focuses on the rolling properties of a specific family of knots: Morton's knots (Morton, 1991). These knots are special, because they are *tritangentless*, meaning any three points on the curve can't share a tangent plane. What this means for rolling, intuitively, is the absence of support planes. With no support planes, the knot can't be stably placed on a surface and is then more likely to roll.

By considering the convex hull of Morton's knots, we can reason about their rolling behavior. The work done in (Eget, Lucas and Taalman, 2020) was to optimize the rolliness of Morton's knots. They found the optimal rolling Morton knot and devised a z-stretch factor, which stretches the z-axis to obtain even lower rolliness measures. Furthermore, in (Dzojic and Kupfer, 2023) was added a horizontal stretching factor, which reduced the rolliness even more. This paper will provide the reasoning behind the effect of these transformations on the rolliness measures. This is achieved by linking the Morton knots to concepts from the TDR family. Additionally, a new transformation is proposed that yields a new family of knots with a rolliness measure of $\rho = 0$. In other words, we obtain a family of smooth rolling knots in the sense that they roll with zero center of mass height variations.

We aren't trying to reinvent the wheel here … or are we? Although this research is purely motivated by mathematical curiosity, there has been a growing interest in robotics for the use of these rolling space curves. For example, imagine a rotating agent, dynamically orienting itself by transforming its defining space curve.

Prerequisite Material

Morton's knots

Formally, a knot is the embedding of S^1 in $\mathbb{R}^3$, *i.e.* closed space-curves. Closure in this case indicates that the curve is a closed loop; it ends where it begins. A (p, q) *torus knot* is a curve defined by it's number of revolutions along the longitudinal and meridional axes of a given torus. It is usually parametrized by an angle ϕ as follows:

$$x(\phi) = (r\cos(q\phi) + R)\cdot\cos(p\phi) \qquad y(\phi) = (r\cos(q\phi) + R)\cdot\sin(p\phi) \qquad z(\phi) = -r\sin(q\phi)$$

where p is the number of revolutions along the longitudinal axis (around the origin), and q along the meridional axis (around the tube), and R, r the torus radii. A *trefoil* is a $(2, 3)$ or $(3, 2)$-torus knot.

Morton's knots are the main character of this paper. They are a special flavor of trefoils, with the property that they are tritangentless. Tritangency is when three points on a curve share a tangent plane. It is the property that makes a tricycle stable, and a bicycle unstable. Since they are guaranteed to never admit a supporting plane, Morton's knots are good candidates for studying the rolling properties of space curves. The knots in question are obtained by the following stereographic projection:

$$x(\phi) = \frac{ca\cos(3\phi)}{1 - b\sin(2\phi)} \qquad y(\phi) = \frac{ca\sin(3\phi)}{1 - b\sin(2\phi)} \qquad z(\phi) = \frac{cb\cos(2\phi)}{1 - b\sin(2\phi)}$$

with $a^2 + b^2 = 1$ and $a, b \neq 0$. This imposed relationship between parameters makes it such that Morton's knots are entirely determined by the value of a. In order to obtain knots that are on the same scale for different values of a, Eget et al. added the extra c scaling parameter, and set it to $c = \frac{a}{1+b}$ such that the torus radii satisfy $R + r = 1$.

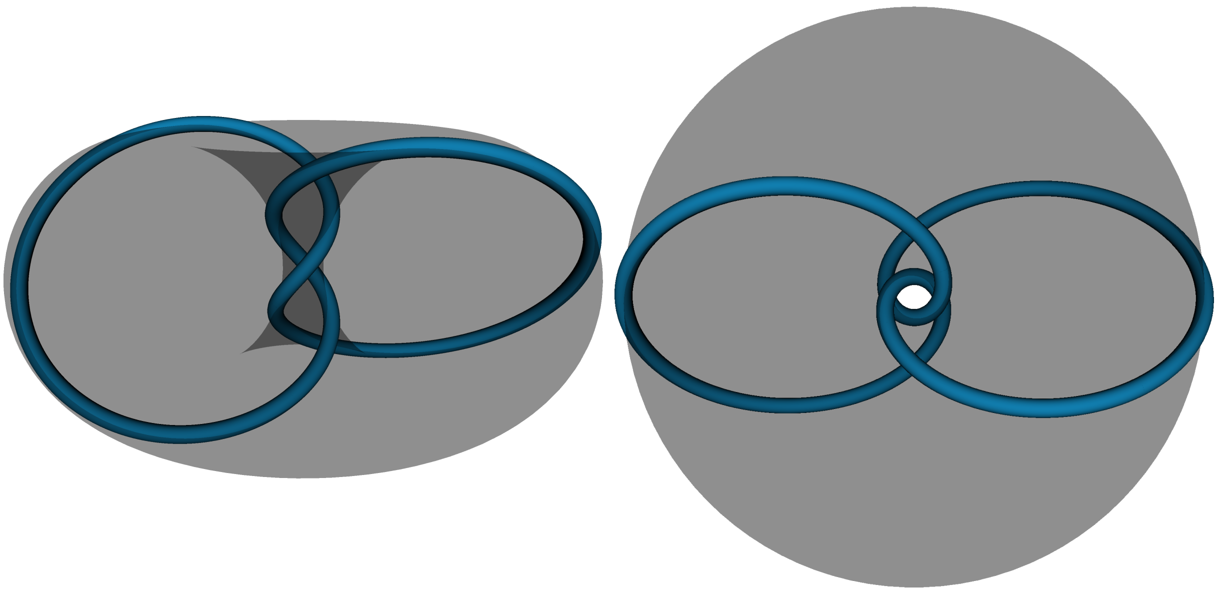

Figure 6: Morton knot with $a = 0.5$

Convex Hull

A *convex hull* is a convex set in $\mathbb{R}^n$, meaning it has the property that for any two of its points, it also contains the line traced between them. The convex hull of a set of points $P \subset R^n$ is the intersection of all convex sets $S \subset \mathbb{R}^n$ such that $P \subset S$.

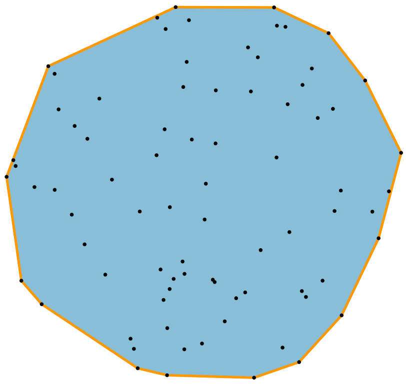

(a) Convex hull (in blue) of a random set of points.

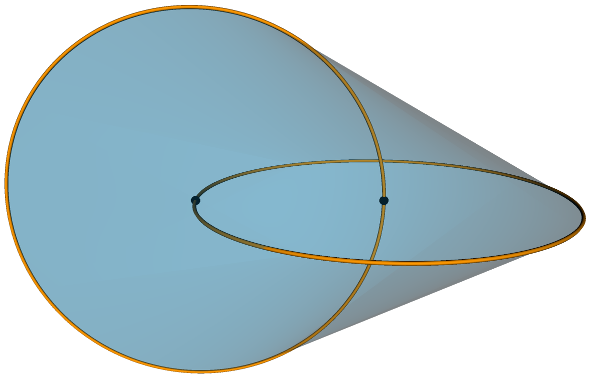

(b) The Oloid is the convex hull of two orthogonal circles passing through each other's centers.

Rolliness ρ

A *rolling trajectory* is the curve on a surface that indicates the path the object traces when rolling. For a sphere, the rolling trajectory would be a circle around the direction it rolls in.

When taking the convex hull of space curves, like the oloid's disks, we obtain a *ruled surface*, meaning any point on the surface lies on a straight line. An obvious example of a surface which is not ruled is the sphere, which has no straight lines. At every instance during the rolling behavior of our ruled surfaces, the contact points with the ground plane are the surface's defining lines. Thus, the rolling trajectory of a ruled surface can be defined as the curve consisting of the lines' midpoints. Figure 1 shows the oloid's rolling trajectory, along with one of its ruled surface lines.

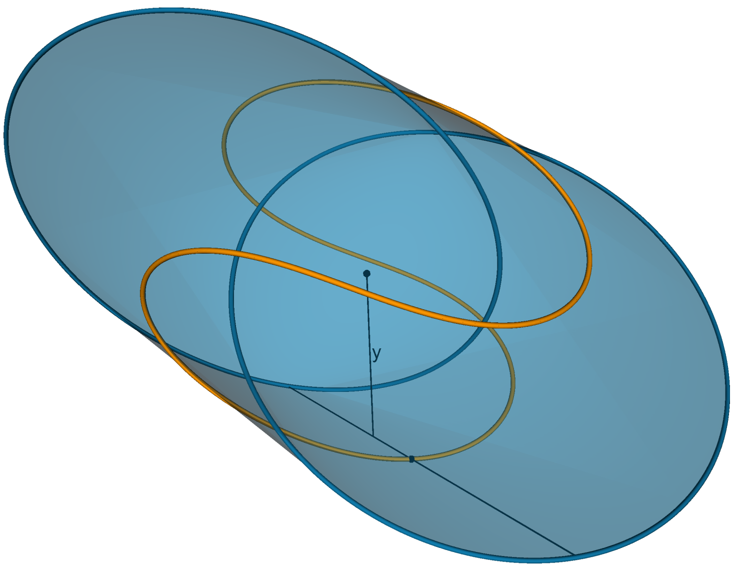

Figure 1: Rolling trajetory of the oloid (orange) and projected center of mass on one of it's trajectory lines.

Rolliness is the metric, denoted by ρ, measuring how smoothly an object rolls. A measure of $\rho = 0$ indicates a smoothly rolling object, such as a sphere. Specifically, the height of the center of mass at every point along the rolling trajectory is considered to measure rolliness. This height is depicted for a specific instance on the rolling trajectory of the oloid in Figure 1. The metric is defined the same way as Eget et al. by the following Range to Average Ratio:

$$\rho = \frac{\max y_{\text{cm}} - \min y_{\text{cm}}}{\overline{y}_{\text{cm}}} \tag{1}$$

where y_{cm} is the projected height of the center of mass of points along the rolling trajectory, and $\overline{y}_{\text{cm}}$ is the mean projected height which is used to obtain a scale invariant metric.

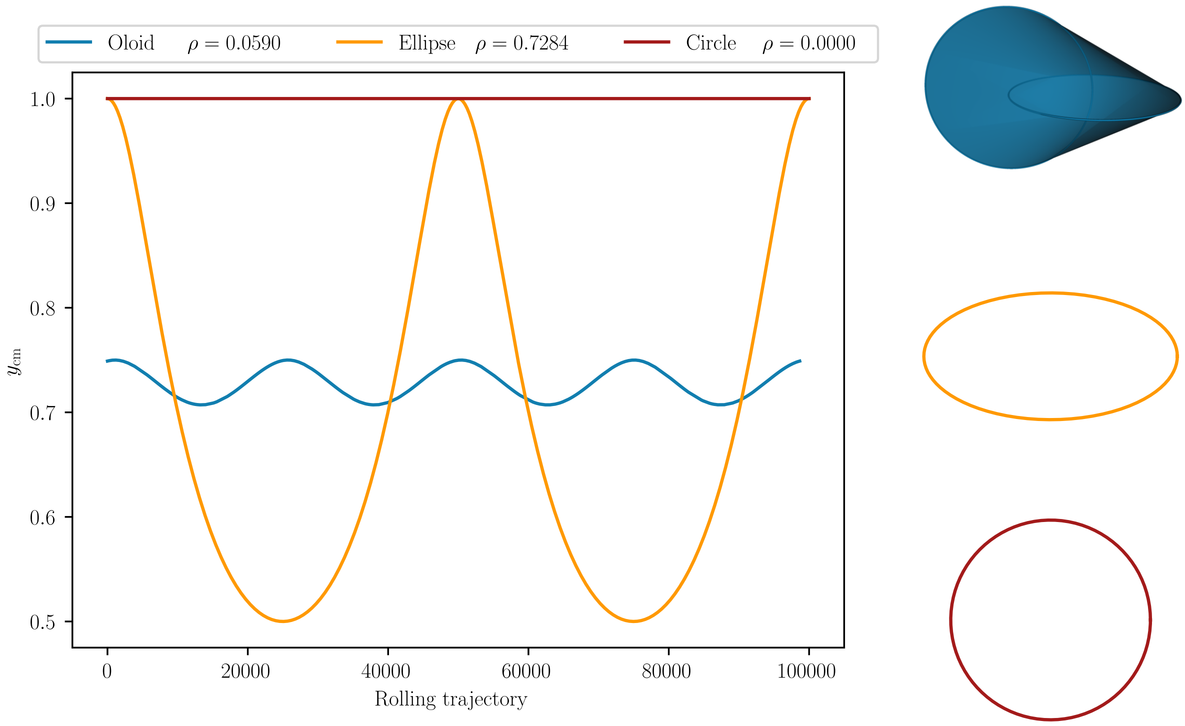

Figure 8: Center of mass height variations of 2D rolling objects and the oloid.

Additional intuition for the rolling behavior of general object's can be gained from reflecting on the objects initial state. The ellipse from Figure 8 is a good example of a rolling object with non-constant center of mass height variations *i.e.* $\rho \neq 0$. If it is initialized on its longer side, then it will not roll. Indeed, it's side is the state in which its center of mass is at its lowest height, corresponding to the bottom of the valleys in Figure 8's height curves. However, if we push it long enough and get it over its tip, it will start rolling. When on its tip, the ellipse is at its center of mass height peak, and when pushed over it, the ellipse will roll continuously if the conservation of energy is respected. Rolliness can be thought of as a metric for this thought process. The higher the rolliness, the longer the push will be to get it over its first center of mass height peak occurence. This checks out for the sphere's zero rolliness value, since virtually no pushing is needed to get it rolling.

Two Disk Roller

A two disk roller is defined as the convex hull of two orthogonal ellipses with radii a, b and a distance between their centers of c. The TDR family has the very useful property that they have $\rho = 0$ when

$$c^2 = 4a^2 - 2b^2 \tag{2}$$

This equation will be continually referred to as the *zero-rolliness condition*, and the family of TDRs satisfying it will be called the *zero-rolliness TDR*s.

Interestingly enough, since circles are ellipses, the oloid is a TDR with $a = b = c = 1$. As shown in Figure 8, the oloid has $\rho \neq 0$. This is in accordance with Equation 2, since the oloid does not satisfy the zero-rolliness condition. However, the oloid can be easily modified to roll smoothly by setting the distance between the circles to $c = \sqrt{2}$.

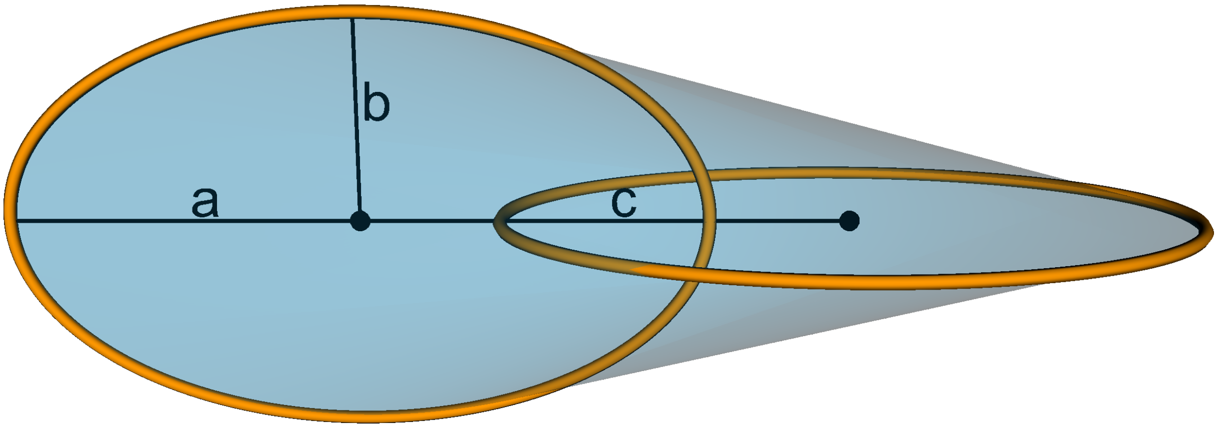

Figure 9: A Two Disk Roller with $a = 0.5, b = 0.3, c = 0.7$

Results

TDR Morton knots

The aim is to transform Morton's knots such that the resulting convex hull is a zero-rolliness Two Disk Roller. But why is it that by matching the convex hull we obtain the same rolliness? This is because the only part of a torus knot contributing to its rolling behavior are the segments that define its convex hull *i.e.* its *exterior*. Due to their symmetry, torus knots have the same center of mass as their convex hulls, which is not necessarily the case for other knots. If this was not the case, the density of the convex hull would need to be considered in order to study the knot's rolliness.

When computing the convex hull of Morton's knots, the resemblance to the good ol' oloid is uncanny. This begs the question: how close is it to the oloid? or a TDR? In order to relate Morton knots to TDRs, we fit disks to the exterior segments of our knots.

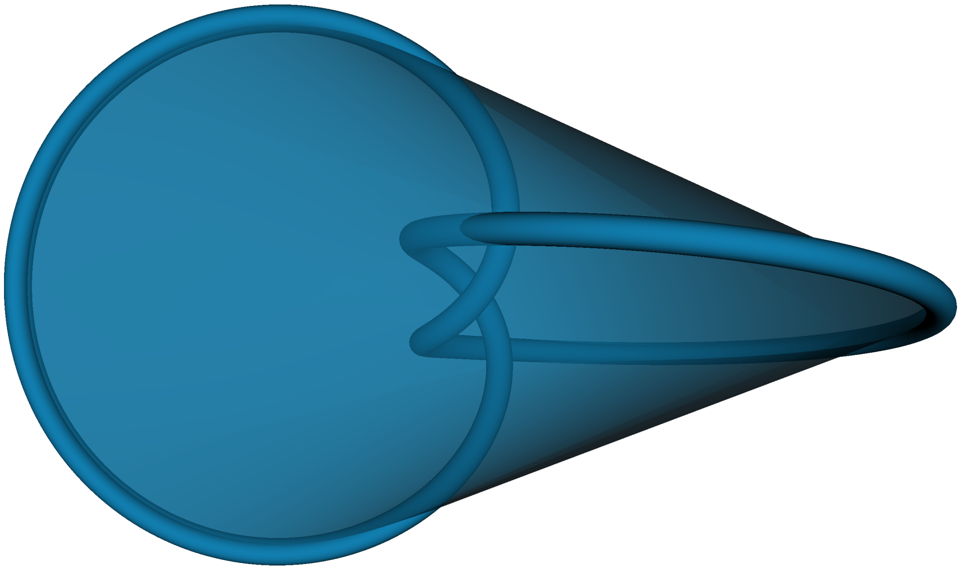

Figure 10: The convex hull of the $a \approx 0.4786$ Morton knot looks like an oloid.

,

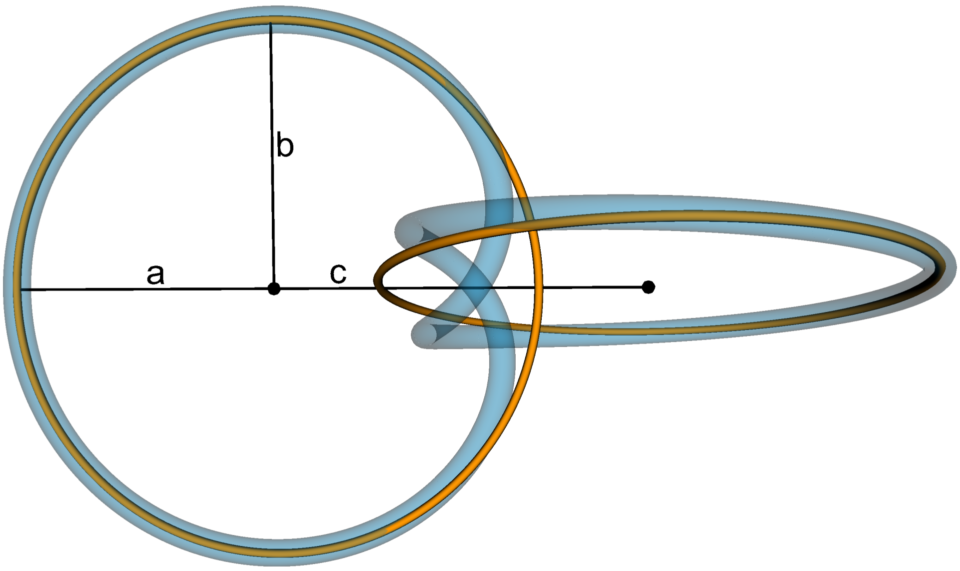

Figure 11: The approximated disks to the $a \approx 0.4786$ Morton knot have a, b, c TDR parameters satisfying the zero-rolliness condition

Intriguingly, when $a \approx 0.4786$, the corresponding Morton knot satisfies the zero-rolliness condition. Indeed, this knot's approximated disks have TDR parameters $a = 0.5876, b = 0.59197$ and $c = 0.82479$ that approximately satisfy Equation 2. But this knot has non-zero rolliness $\rho = 0.2509$. So how could this be?

Well, the thing is, the convex hulls of these approximated disks are not TDRs. To be a TDR is to be defined by orthogonal disks, meaning the planes they lie in are defined by orthogonal vectors. This is not the case for the Morton knot satisfying the zero-rolliness condition. In fact, exactly one Morton knot has orthogonal approximated disks: the $a = 0.5831$ Morton knot. Coincidentally, this is the a value for the smoothest rolling Morton knot (minimal ρ) found in (Eget, Lucas and Taalman, 2020). This is strong evidence as to why no Morton knot rolls smoothly: the unique Morton knot satisfying the zero-rolliness condition does not coincide with the unique Morton knot with orthogonal approximated disks.

Eget et al. further introduced a z-stretching factor that helped reduce the rolliness of the other, non-orthogonal-disk-having knots. Now instead of this convoluted name, let's refer to the family of Morton knots with orthogonal approximated disks as the *TDR Morton knots*, since their convex hulls are TDRs. The main discovery of this section is that the optimal z-stretching factor corresponds to a scaling factor leading to orthogonal approximate disks, as shown in Figure 12. These optimal z-stretched knots thus populate the TDR Morton knot family.

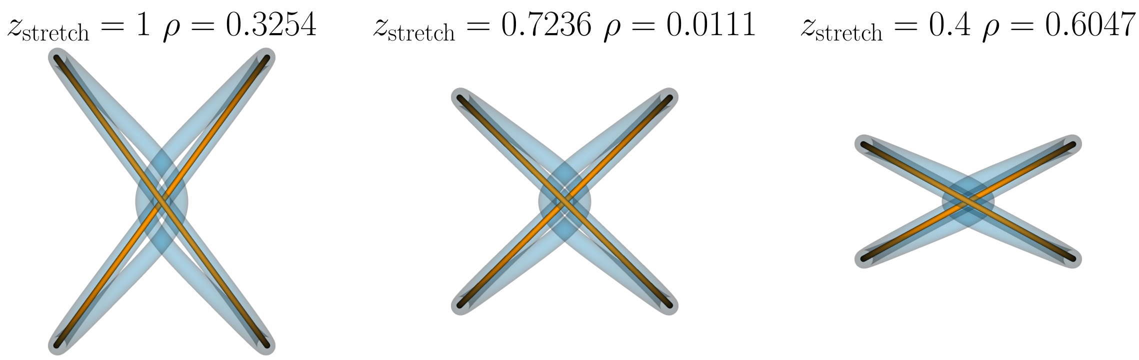

Figure 12: Optimizing z_{stretch} of the $a = 0.45$ Morton knot for ρ gives orthogonal disks. The middle knot is a member of the TDR Morton knot family.

The next observation is that no TDR Morton knot has TDR parameters satisfying the zero rolliness condition from Equation 2. This is good intuition as to understanding why (Eget, Lucas and Taalman, 2020) did not obtain perfectly smooth rolling Morton knots.

Zero-rolliness TDR Morton knots via TDR projections

The previous section was about the z_{stretch} transformation that yields orthogonal approximate disks, and defines the TDR Morton knot family: a class of knots with TDR convex hulls. Therefore, applying a transformation to a TDR knot to obtain a zero-rolliness TDR convex hull yields a smooth rolling knot!

The method starts with the TDR knot's approximated disks. A value of c satisfying the zero-rolliness condition from Equation 2 is computed by using the a, b ellipse radii of the approximated disks. These three parameters thus define a zero-rolliness TDR, and all that is left is to project the TDR knot to the zero-rolliness TDR disks. For this, a computational approach is used, in which the exterior points are matched exactly to their closest point on the zero-rolliness TDR disks. A decaying translation is applied to the interior points to preserve continuity.

We note that the projection to the zero-rolliness TDR disks is mostly a “horizontal stretch” in the axis of the knot’s maximum width in the xy plane, and thus explains why a horizontal scaling improved rolliness values in (Dzojic and Kupffer, 2023).

Figure 15 shows that the resulting projected knot has the lovely smoothness property of $\rho = 0$, and will be referred to as a zero-rolliness TDR Morton knot.

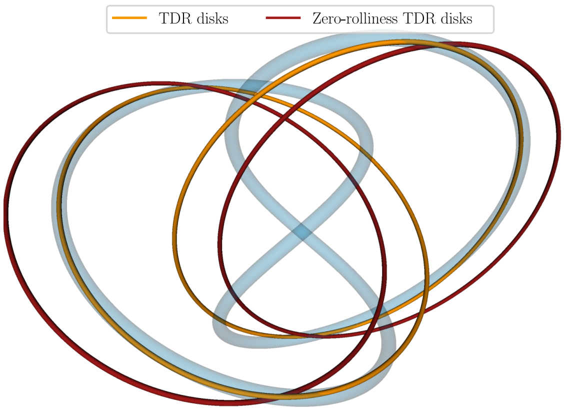

Figure 13: The zero-rolliness TDR disks with the same ellipse radii as the $a = 0.8$ TDR knot’s approximated disks.

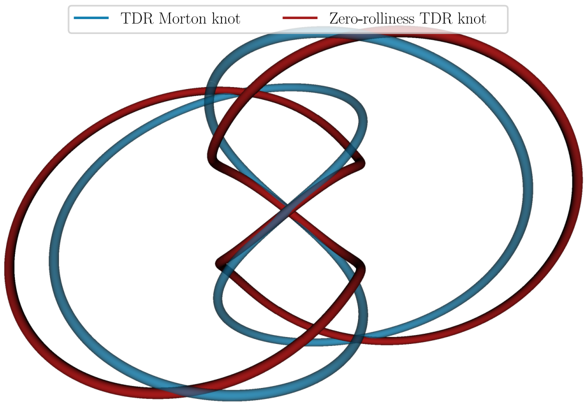

Figure 14: The stretched $a = 0.8$ Morton knot projected to zero-rolliness TDR disks.

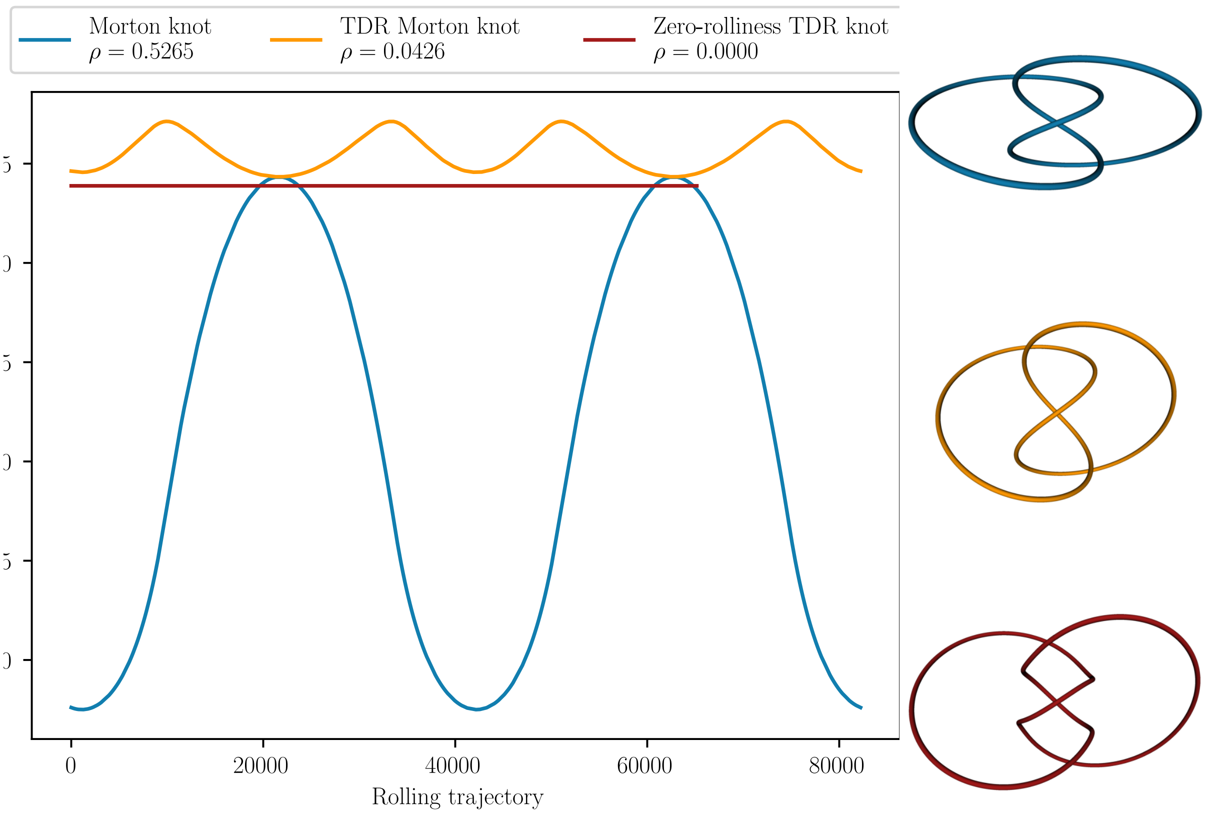

Figure 15: The projected knot has no center of mass height variations.

In fact we can apply this projection method to all TDR Morton knots, and it indeed yields an entire family of smooth rolling knots.

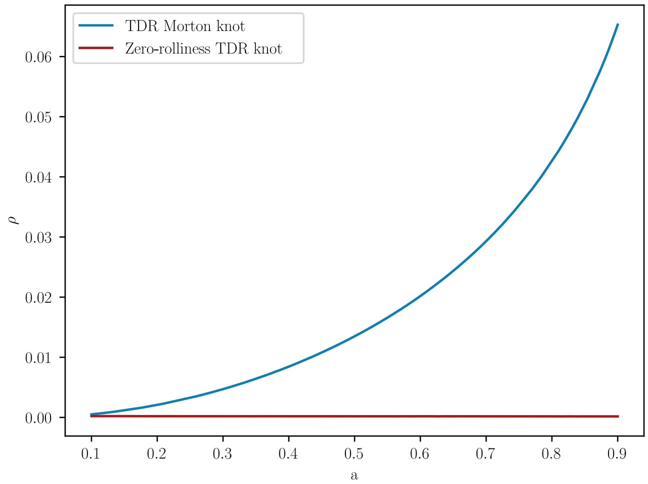

Figure 16: Rolliness of the TDR Morton knots and zero-rolliness TDR Morton knots which indeed have zero-rolliness.

Simulation

The projection method is validated through simulation. To simulate rolling knots, we place them on a slightly tilted plane to provide a directed force to initiate the rolling. Additionally, depending on the knot, a larger initial force is required to nudge them over their center of mass peak.

It is found through simulation that the projected knot does not require a larger initial force to begin it's rolling behavior, whereas both the base and stretched knots require forces with magnitudes of around 14N and 11N for a duration of 20 and 10 simulation frames to get over their center of mass height peaks.

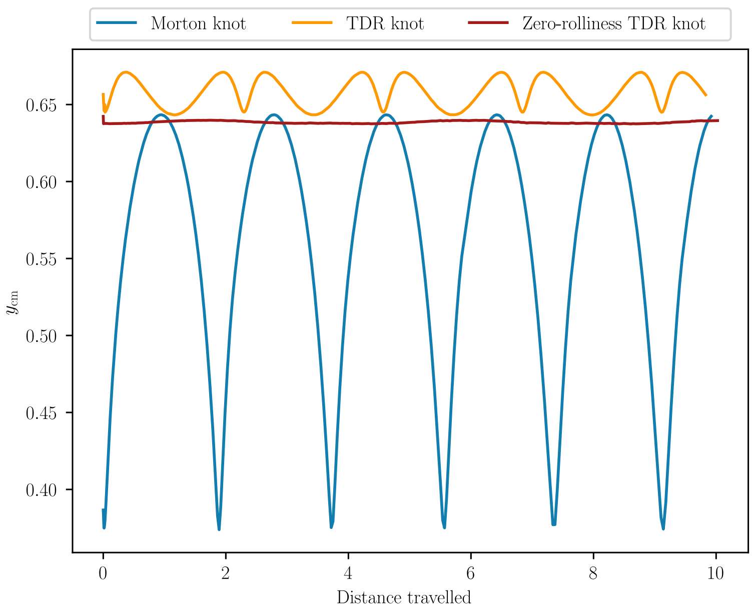

Figure 17: Simulated height variations of Morton knots with $a = 0.8$.

The previously mentioned peaks can be seen in Figure 17, and the initial force is the one needed to push the knot over their first occurence. The projected knot has no initial hill, and thus requires no initial force. The small kink is because the knot is initialized slightly higher than needed, and thus is in free fall until hitting the plane. The slight deviation in the projected knot height curve is due to the knot's discretization and Blender's collision detection. A much lower knot resolution is required to obtain a decent running time for Blender simulations.

Generalized Morton knots

In (Eget, Lucas and Taalman, 2020) it was mentioned that to roll, a knot need only be externally tritangentless. This means dealing with Morton's knots is overkill, since we don't require these knot to be tritangentless everywhere, but only on the exterior. By taking values of $p > 3$ odd, we obtain a generalization of Morton's knots, which appear to have this property.

The value of $q = 2$ is mandatory for torus knots to roll, since any more would yield external tritangents. One can visualize this by placing the torus flat on a support plane. The intersection of the plane and the torus draws a circle on the plane, and corresponds to the lowest parallel line on the torus. A (p, q)-torus knot crosses this lowest parallel exactly q times. Even more, the support plane is in fact tangent to these points. If $q > 2$, then the knot would wrap around the tube more than twice, and thus cross the lowest parallel more than twice, making the support plane a tritangent.

We can apply the same z-stretching optimization to obtain new TDR Morton knots, and improved rolliness values.

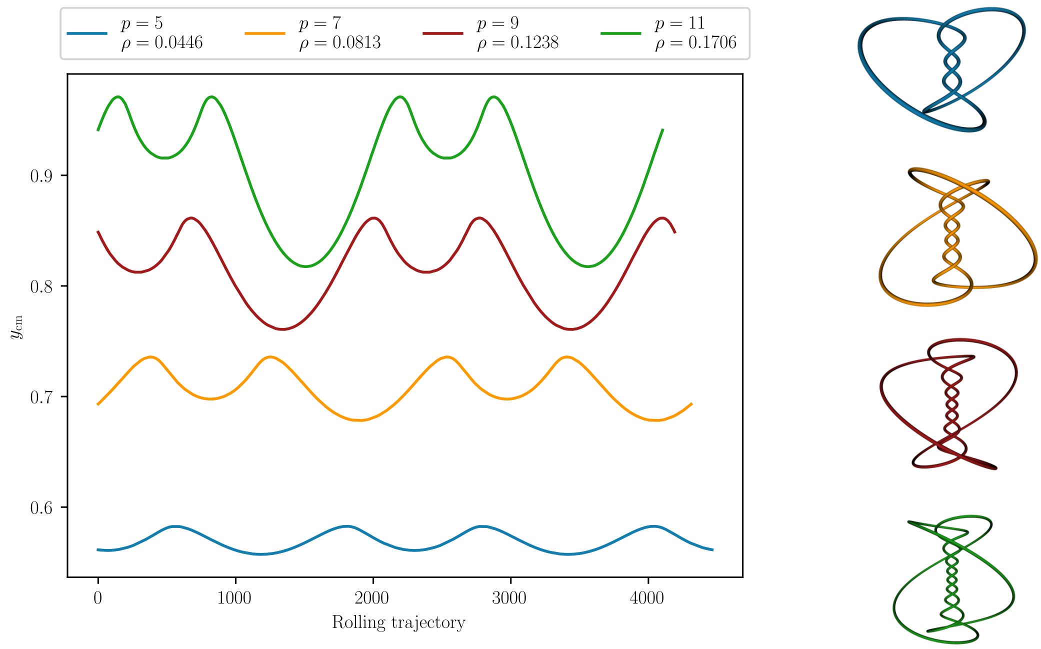

Figure 19: Height variations along the rolling trajectory of generalized TDR Morton knots.

As p increase, it becomes less clear how these knots are related to Two Disk Rollers. But the increase in complexity makes the rolling trajectory of these knots particularly intriguing.

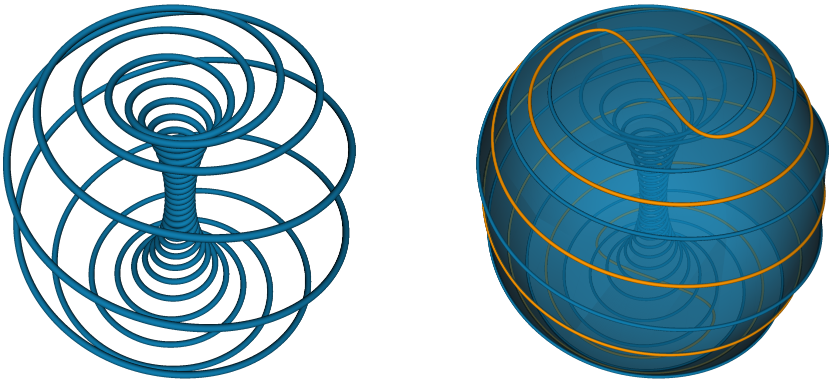

Figure 20: The $p = 31$ generalized $a = 0.8$ TDR Morton knot and its rolling trajectory.

Finally, by following the same reasoning as before, the projection method can be applied to these new knots. For $p = 5$, the projection successfully yields a generalized zero-rolliness TDR knot while preserving the topology (see Figure 21). Simulation of this knot confirms its rolliness properties.

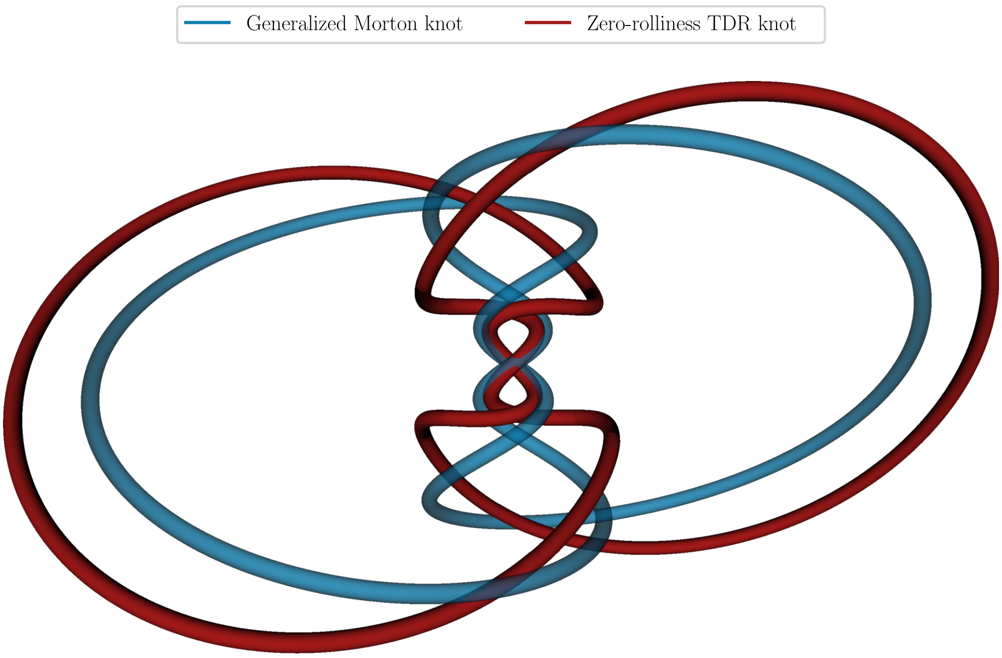

Figure 21: Projected $p = 5$ generalized Morton knot with $a = 0.5$

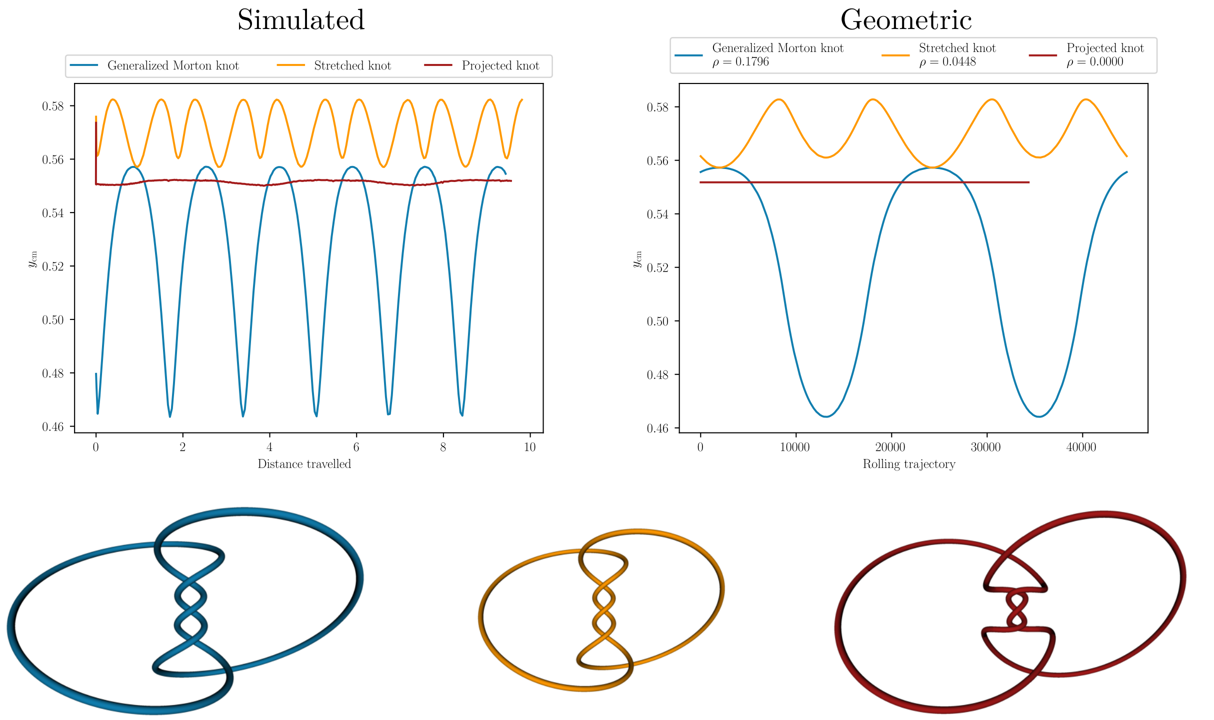

Figure 22: Geometric and simulated center of mass height variations for the $p = 5$ generalized Morton knot.

However, for $p \geq 7$, the projection method breaks. Although the resulting knot still has zero rolliness, the topology of the base knot is lost because of self intersections during the projection.

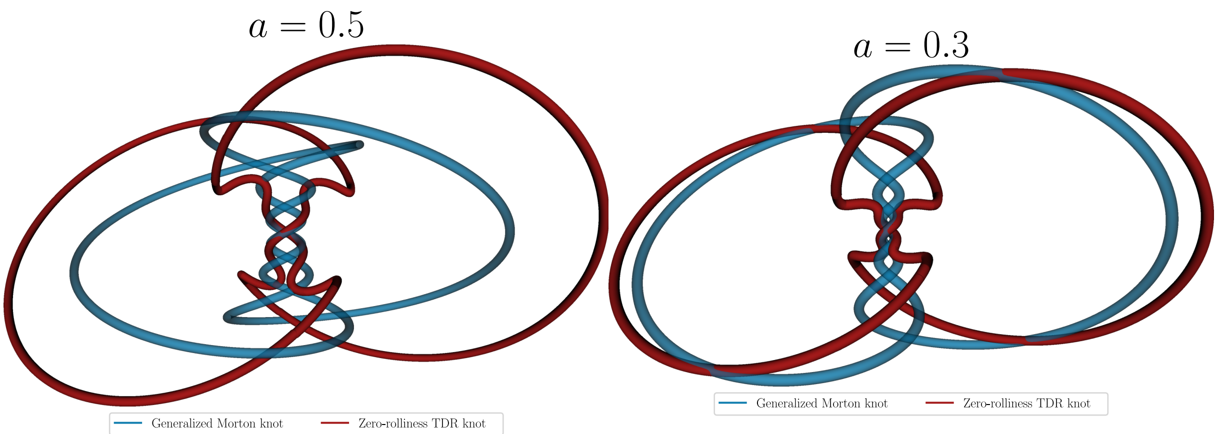

Figure 23: The projection method breaks for $p \geq 7$ generalized Morton knots due to self intersections.

Conclusion

The smoothest rolling Morton knot from (Eget, Lucas and Taalman, 2020) corresponds to the unique instance in the Morton knot family with orthogonal approximate disks. The effect of the Eget et al.'s z-stretch is of modifying the angle between the approximated disks, and obtaining orthogonal disks in rolliness optimality. The TDR Morton knots are the family of optimally z-stretched knots with orthogonal approximate disks. However there is no TDR Morton knot satisfying the zero-rolliness condition. Projecting the TDR Morton knots to zero-rolliness TDR disks by means of a decayed translation yields a class of smooth rolling knots. Further, since an object only needs to be externally tritangentless to roll, one can generalize the Morton knots to obtain new rolling knots with higher complexity. These generalized knots can be z-stretched as well, which improves the rolliness, but the projection method can only be applied for the $p = 5$ generalized knot, since the method does not preserve the topology for higher p values.

There remain many un-answered questions: What do the optimized parameter values, such as $a = 0.5831$ represent analytically? Is there a closed formula to express a surface's center of mass height variations? Are all generalized Morton knots externally tritangentless? Also, there must be a better projection method to preserve the topology of higher p valued generalized knots. Furthermore, one could use a curve energy to smoothen out the projections.

Bibliography

Dzojic, Matilde Sciortino and Kupffer, P. (2023) "Rolling Knots"

Eget, A., Lucas, S. and Taalman, L. (2020) "Optimizing Morton's Tritangentless Knots for Rolling," in

Engelhardt, C. and Ucke, C. (2017) "The Two-Disc-Roller – a Combination of Physics, Art and Mathematics," in. Available at: https://api.semanticscholar.org/CorpusID:207986461

Hirsch, D. and Seaton, K. A. (2020) "The polycons: the sphericon (or tetracon) has found its family," *Journal of Mathematics and the Arts*, 14(4), pp. 345–359. Available at: https://doi.org/10.1080/17513472.2020.1711651

Morton, H. R. (1991) "Trefoil Knots without Tritangent Planes," *Bulletin of the London Mathematical Society*, 23(1), pp. 78–80. Available at: https://doi.org/10.1112/blms/23.1.78